Potassium Radical Anion Salts of 2,3-Bis(2-Pyridyl)quinoxaline

Andrew S. Ichimura, Lawrence P. Szajek, Qingshan Xie, Rui H. Huang, Song Z. Huang, Michael J. Wagner, James L. Dye,* and James E. Jackson*

Department of Chemistry and Center for Fundamental Materials Research, Michigan State University, East Lansing, Michigan 48824-1322

Received: October 7, 1998

Alkali metal radical anion salts in which the cations are coordinated directly by the radical anions have been studied extensively in solution, but relatively little in the solid state. We have prepared and characterized two such salts from 2,3-bis(2-pyridyl)quinoxaline (dpq) and potassium metal at −60 °C and 10^{-5} Torr. Crystals from THF show a zig-zag contact ion pair chain structure whereas a dimeric structure is obtained from methylamine. In both systems, the potassium ions occupy sites consisting of four quinoxaline nitrogens and solvent molecules. These salts have been further characterized by thin-film and solution optical spectroscopy, solution EPR and ENDOR spectroscopies, magnetic susceptibility, and cyclic voltammetry measurements.

Introduction

Radical anions generated by electron transfer reactions are important intermediates in organic and inorganic chemistry.[1] Due to their high reactivity, alkali metal radical anion salts in which the cations are directly coordinated to the radical anion (and not a solvent-separated pair) have been studied extensively in solution, but relatively little in the solid state. For example, the sodium pyrenide radical anion salt[2] and the radical anion sodio-cryptatium[3] have been studied in solution and structurally characterized by X-ray diffraction, but no other solid state properties were reported. We have prepared and characterized in solution and in the solid state two highly reactive and temperature sensitive radical anion salts from 2,3-bis(2-pyridyl)-quinoxaline (dpq) and potassium metal at −60 °C and 10^{-5} Torr. During the course of this study, Bock and co-workers published X-ray structures for the sodium and potassium radical anion salts of the parent compound 2,3-diphenylquinoxaline.[4]

Results

The quinoxaline system (dpq) (Scheme 1), a well-known electron accepting ligand,[5] was readily reduced by alkali metals in solution and electrochemically. The cyclic voltammogram of dpq in THF (Figure 1) shows one reversible reduction potential at −1.95 volts with respect to the Fc^+/Fc (Fc = ferrocene) couple and irreversible reduction waves at −2.84, −3.00, and −3.14 volts. A single electron reduction at −1.64 volts vs SCE in acetonitrile had been reported earlier.[6] The optical spectrum of the dpq monoanion was obtained after reduction with one equivalent of potassium metal in a modified K-cell[7] fitted with a thin quartz optical cell. The optical spectrum from 0.4 to 1.7 microns, Figure 2, shows little change between a THF solution and the thin film left upon solvent evaporation.

SCHEME 1

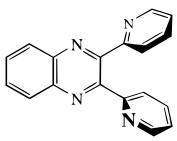

(**dpq**)

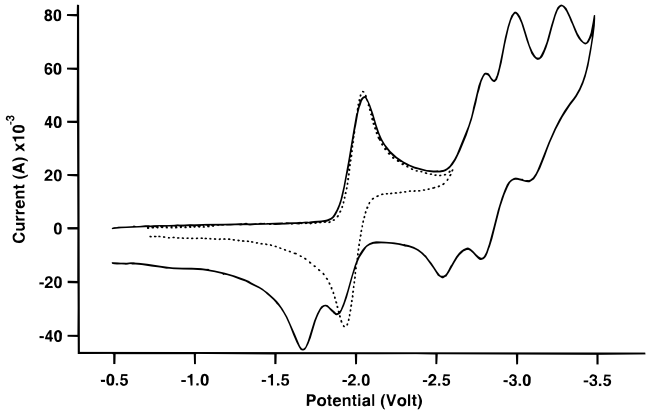

Figure 1. Cyclic voltammogram of dpq in THF at room temperature showing a reversible one electron reduction (dashed line) and an irreversible multielectron reduction (solid line).

A THF solution of dpq has no absorptions in this region. The intense visible absorptions at 0.42 and 0.58 microns and the broad absorption at 1.2 microns can be attributed to the alkali metal cation−radical anion contact ion pair in solution. The tendency of the dpq pyridine and pyrazine nitrogen atoms to coordinate alkali metal cations was illustrated by the observation of dramatic ^{1}H NMR shifts in the aromatic region when incremental amounts of NaI were added to neutral dpq in deuteroacetone. The ^{1}H-NMR spectra are included in the Supporting Information.

By utilizing standard low temperature and high vacuum techniques for the preparation of air and temperature sensitive compounds,[7] we prepared in good yield two radical anion salts of dpq. Crystals of $K[(dpq)](THF)_2$ and $K[(dpq)](MeNH_2)_3$ were obtained when potassium mirrors and dpq were allowed to react at −60 °C in THF and methylamine, respectively.

As a reference point for the description of the crystal structures below, it is noted that in the free dpq ligand the nitrogens on both pyridine rings are rotated toward the center.[8] The torsional angle about the carbon−carbon bonds connecting the pyridine rings to the quinoxaline ring is 30.3°.[8]

X-ray structure analyses of $K[(dpq)](THF)_2$ and $K[(dpq)](MeNH_2)_3$ revealed that in both systems the potassium cations

10.1021/jp983994c CCC: $15.00
Published on Web 12/09/1998

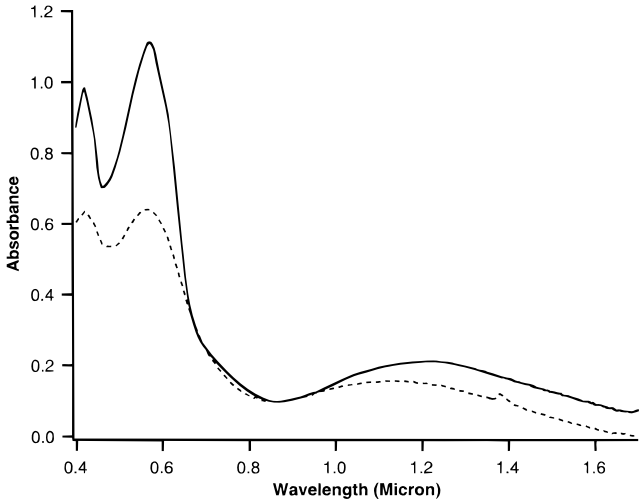

Figure 2. Optical spectra of dpq reduced with 1 equiv of potassium metal at −60 °C and 10^{-5} Torr. (a) Spectrum of monoanion in THF (solid line). (b) Spectrum of monoanion after solvent evaporation (dashed line).

are coordinated to the dpq nitrogen atoms and solvent molecules. Both compounds appear as small blocky crystals that are dark purple in color. Crystals of K[(dpq)](THF)$_2$ are orthorhombic in the space group, *Pca*2$_1$. The cations and anions form linear chains with the motif, -K$^+$dpq$^-$K$^+$dpq$^-$-, such that the cation coordinates to the pyrazine and the pyridine nitrogen lone pairs of adjacent dpq anions. Two THF molecules complete the pseudo-octahedral coordination sphere of each K$^+$. A fragment of the crystal structure with the linear chain arrangement is illustrated in Figure 3. The nearest distance between chains, measured as the distance between K$^+$ cations, is approximately 11 Å. One notable change between the radical anion ligand and the neutral free ligand is that each pyridine ring has "flipped", allowing chelation to the metal center. The torsional angles between the carbon−carbon bonds connecting the pyridine rings to the quinoxaline ring are 22° and 36°, only slightly different from the torrsional angle in the free ligand (30.3°).[8] The average pyridine nitrogen−K$^+$ and quinoxaline nitrogen−K$^+$ distances are 2.88 and 2.95 Å, respectively. A similar linear chain arrangement of contact ion pairs was reported for K$^+$[2,3-diphenylquinoxalide](MeOCH$_2$CH$_2$OMe) with an average nitrogen−K$^+$ distance of 2.8 Å.[4]

Crystals of K[(dpq)](MeNH$_2$)$_3$ are monoclinic in the space group $P2_1/c$. dpq forms contact ion pair dimers when crystallized from methylamine solution. The dimeric unit is illustrated in Figure 4 in which the K$^+$ and dpq$^-$ nitrogen atoms are labeled by their atomic symbols, while the nitrogen atoms from the solvent are unlabeled. The contacts between K$^+$ and the closest nitrogen atoms are illustrated as bonds. Inspection of Figure 4 reveals that each K$^+$ ion has a 7-fold coordination sphere consisting of four nitrogen atoms from two dpq anions (one quinoxaline and one pyridyl nitrogen from each dpq$^-$) and three nitrogen atoms from solvent molecules. Interestingly, the structure has a short K$^+$ to K$^+$ distance of 3.56 Å. Both K$^+$ ions share the same four dpq$^-$ nitrogen atoms by lying above and below the plane defined by the nitrogen atoms (these N atoms are coplanar to within ±2°). The, average distance from each K$^+$ to the dpq nitrogen atoms is 2.99 Å but the individual distances vary from 2.86 to 3.17 Å. The average distance separating the K$^+$ ions from the three amine nitrogens is 2.9 Å. In each dpq molecule of the dimer, one pyridine ring is twisted by ∼28 degrees out of the least-squares plane defined by the quinoxaline ring. The nitrogen atom of this ring coordinates to two K$^+$ cations. The other pyridine ring is twisted by ∼51° and the nitrogen atom points in toward the center of the dimer. The pyridine nitrogen atom of the latter ring is only 3.1 Å away from one of the methylamine nitrogen atoms and probably forms a hydrogen bond to this solvent molecule as shown in Figure 4.

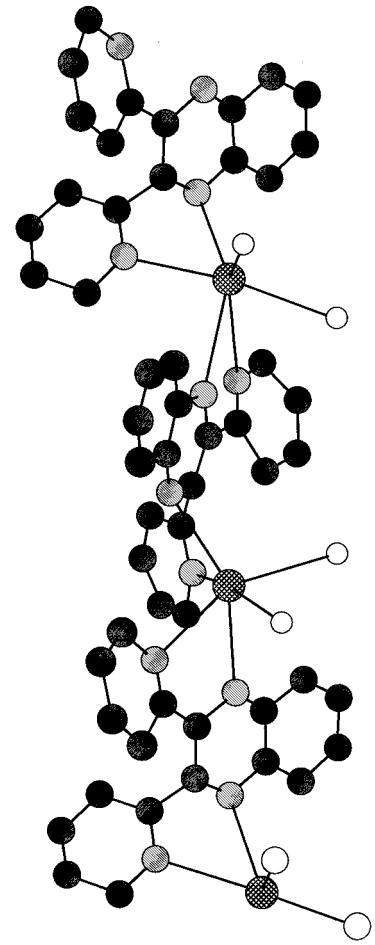

Figure 3. Part of the K[(dpq)](THF)$_2$ crystal structure showing the linear chain arrangement of contact ion pairs. The carbon atoms of the THF molecules were removed for clarity leaving only the oxygen atoms (open circles).

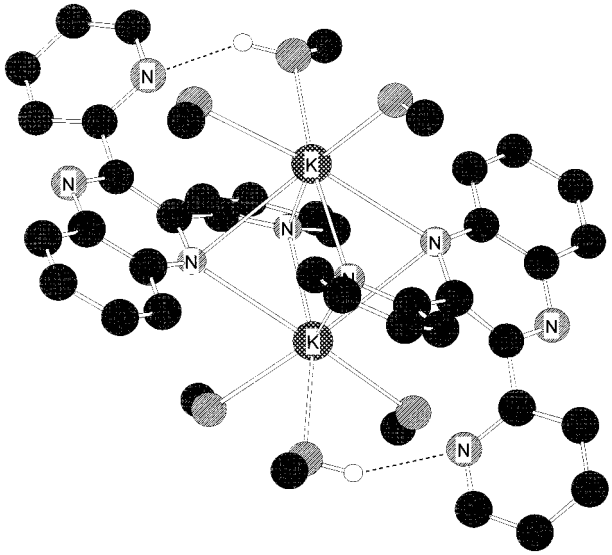

Figure 4. Part of the K[(dpq)](MeNH$_2$)$_3$ crystal structure showing the dimeric nature of the contact ion pairs.

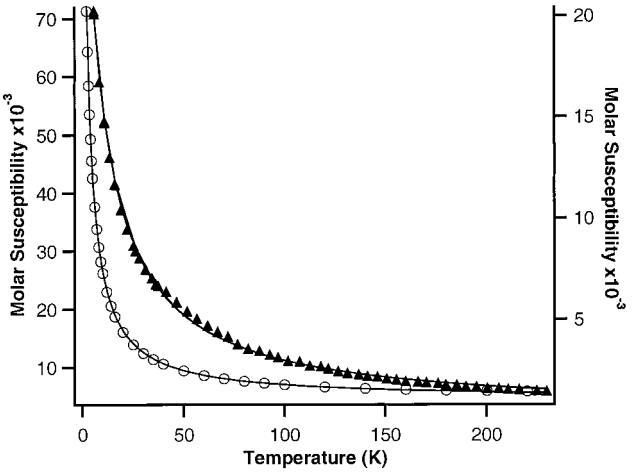

Figure 5. Plot of molar susceptibility χ_m vs temperature for K[(dpq)](THF)$_2$ (triangles, left ordinate) and K[(dpq)](MeNH$_2$)$_3$ (open circles, right ordinate).

TABLE 1: Crystallographic and Refinement Data for K[(dpq)](THF)$_2$ and K[(dpq)](MeNH$_2$)$_2$

	K[(dpq)](THF)$_2$	K[(dpq)](MeNH$_2$)$_3$
space group	orthorhombic, $Pca2_1$	monoclinic, $P2_1/c$
cell-parameters		
a, Å	15.843(15)	16.153(5)
b, Å	20.2418(77)	14.613(5)
c, Å	14.8763(52)	18.989(6)
β, degrees		95.38(3)
z	4	4
crystal dimensions, mm	0.3 × 0.4 × 0.4	0.25 × 0.25 × 0.2
scan type	ω	ω
maximum 2θ	45°	45°
temperature (K)	198	200
no. of reflections collected	3533	7161
no. of unique reflections	3283	5881
no. of reflections used in refinemt. with $F_0^2 > 2\sigma(F_0^2)$	2101	2249
no. of variables	275	523
R	0.184	0.026
R_w	0.503[a]	0.058
high peak in final diffraction map, e/Å^3	3.66	0.35

[a] Refined on F^2.

Crystallographic data and data collection parameters for both structures are given in Table 1. Atomic positional parameters for K[(dpq)](THF)$_2$ and K[(dpq)](MeNH$_2$)$_3$ are given in the Supporting Information.

The magnetic susceptibility of both crystalline salts, K[(dpq)](THF)$_2$ and K[(dpq)](MeNH$_2$)$_3$, were recorded in the temperature range 2−300 K. Plots of χ_m versus T (K) for K[(dpq)](THF)$_2$ and K[(dpq)](MeNH$_2$)$_3$ are displayed in Figure 5. The solid lines in Figure 5 represent the least squares fit of the magnetic susceptibility data to a Curie−Weiss model of paramagnetic behavior. The Weiss constants for the two salts were found to be $\theta = -11.8$ K and $\theta = -1.8$ K for K[(dpq)](THF)$_2$ and K[(dpq)](MeNH$_2$)$_3$, respectively.

The EPR spectrum of dpq$^-$ in THF solution (∼1−2 mmol) at 257 K prepared by reduction with one equivalent of potassium metal is shown in Figure 6a. The interaction of the unpaired electron with two equivalent pyrazine nitrogen atoms produces five hyperfine splitting (hfs) lines that dominate the spectrum, while the hfs due to the remaining nuclei is superimposed over the $m_I = 0, \pm1, \pm2$ transitions. At temperatures below 240 K, the line width of the pyrazine nitrogen $m_I = \pm1, \pm2$ transitions increases due to viscosity induced rotational broadening. The

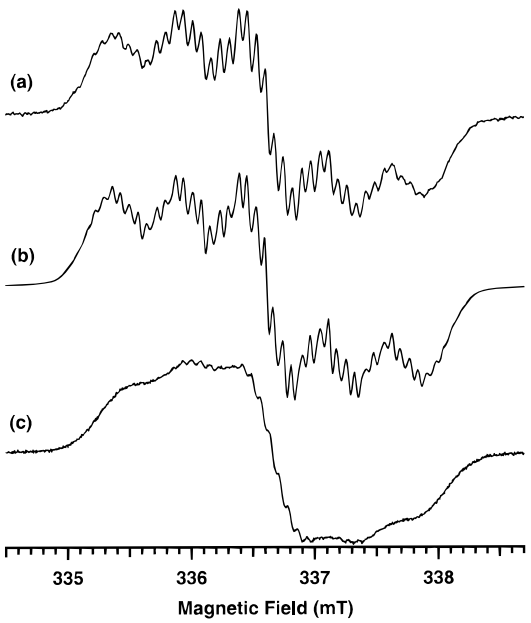

Figure 6. EPR spectrum of dpq monoanion in THF solution (a) at 257 K, (b) simulation, and (c) at 233 K with 1 equiv of cryptand-[2.2.2] present in solution.

EPR spectrum was simulated, Figure 6b, with hfs constants determined from proton electron−nuclear double resonance spectroscopy (^{1}H-ENDOR) and by adjusting the nitrogen hfs constants by a nonlinear least-squares procedure. Details of the calculation are described below. When the K$^+$ selective cryptand[2.2.2] (C222) is added to a THF solution of dpq$^-$ prepared by reduction with potassium metal, the contact ion-pairs separate into "free" dpq$^-$ and cryptated K$^+$ ions. Cryptated K$^+$ can still associate with dpq$^-$ to form ion pairs (in this case, "solvent" or "cryptand" separated ion pairs) in solution, but the ability of the cryptated cation to chelate the dpq$^-$ nitrogen atoms is significantly reduced. Henceforth, the expression "free" ion refers to dpq$^-$ in solution that also contains C222 to break up the tight contact ion pairs. The hfs of the EPR spectrum of free dpq$^-$ (Figure 6c) is poorly resolved compared to the spectrum of the contact ion-pair.

In order to determine the isotropic hfs constants of dpq$^-$, ^{1}H-ENDOR measurements were carried out on the THF solutions with and without cryptand[2.2.2] present in solution. ENDOR spectra of the free dpq$^-$ anion (with C222) and ion paired (no C222) with K$^+$ show four and six distinct hfs resonances at 170 and 178 K, as shown in Figures 7a and b, respectively. At higher temperatures, only four ^{1}H-hfs signals are observed so that the ENDOR spectrum of the contact ion pair at 243 K, Figure 7c, is nearly identical to that of the free ion at 170 K. The ^{1}H-ENDOR spectra of the free ion and the contact ion pair measured at 170 K and 243 K, respectively, closely resemble the ENDOR spectrum of diphenylquinoxaline obtained by Bock et al. at 200 K.[4]

The measured values of the proton hfs constants are summarized in Table 2 and assigned as shown in Scheme 2. At 243 K, the two largest hfs constants, 0.211 and 0.147 mT, can be assigned to the quinoxaline protons $H_{5,8}$ and $H_{6,7}$, respectively, by comparison to other quinoxaline derivatives.[4,9] Notice that these values are exactly intermediate between the values observed at 178 K in THF. The hfs of protons $H_{5,8}$ and $H_{6,7}$ for the free ion, 0.222 and 0.144 mT, respectively, differ only slightly from those of the contact ion pair. Only two other proton hfs constants were observed by ENDOR spectroscopy, whereas up to four proton hfs constants might be expected for the

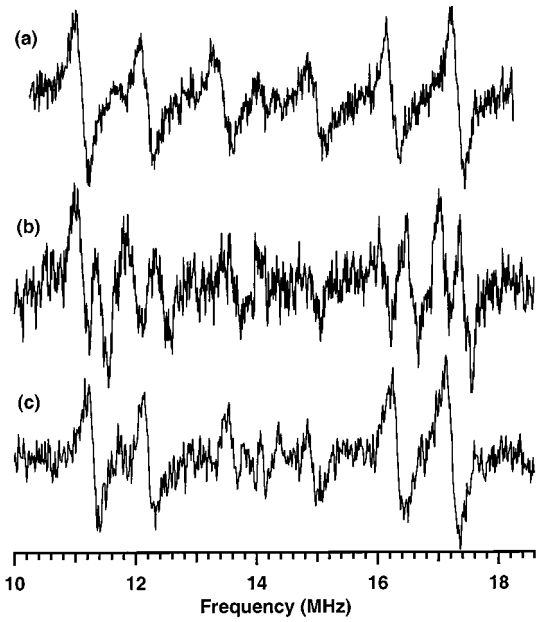

Figure 7. Solution ENDOR spectra of dpq in THF reduced with K metal (a) at 170 K with one equivalent of cryptand[2.2.2] present in solution, (b) at 178 K (no C222), and (c) at 243 K (no C222).

TABLE 2: Isotropic Hyperfine Splitting Constants (hfs) of dpq Determined from ENDOR Measurements and Simulation of the EPR Spectrum

	experimental hfs constants from ^{1}H-ENDOR in mT			fitted
	THF	THF	THF with C222	parameters
temperature (K)	243	178	170	
$H_{5,8}$	0.211	0.224,0.204	0.222	
$H_{6,7}$	0.147	0.163,0.131	0.144	
$H_{a,c}$	0.046	0.045	0.056	
$H_{b,d}$	0.013		0.01	
N(quin)				0.515
N(pyridyl)				0.075
H_c				0.052

SCHEME 2

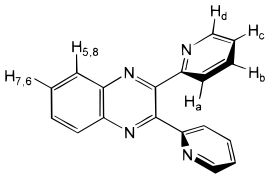

pyridine ring. We assign the 0.056 mT coupling to the ortho and para protons ($H_{a,c}$) and the <0.001 mT coupling to the meta protons ($H_{b,d}$) of the free ion. The two smallest hfs constants observed for the contact ion pair, 0.046 and 0.0013 mT, are similarly assigned. However, a better fit to the observed EPR spectrum can be obtained if the two protons $H_{a,c}$ in the contact ion pair are assigned slightly different values as will be described below.

The experimental ^{1}H-hfs constants were used as input to a program that simulates solution spectra up to fourth order. The solution EPR program was then introduced as a function into the general nonlinear least-squares fitting program KINFIT.[10] KINFIT varies the undetermined hfs constants, line width, *g*-value, and other parameters that scale the simulation appropriately until the weighted sum of the squares of the residuals is a minimum. The dpq pyrazine and pyridine nitrogen hfs constants were determined in this way to be 0.515 and 0.075 mT, respectively. Inspection of the residuals, however, indicated a small systematic error. The line shape of the ENDOR resonances at 13.48 and 15.03 MHz of the free ion, Figure 7a, show that the hfs constants of the two protons $H_{a,c}$ are accidentally degenerate (as are protons $H_{b,d}$). However, the pyridine protons $H_{a,c}$ and $H_{b,d}$ are strictly inequivalent because the nitrogen atom is in a position ortho relative to the 2 and 3 positions of quinoxaline. The lineshape of the corresponding resonances in Figure 7c suggests that the accidental degeneracy is lifted in the contact ion pair. The fit to the solution EPR spectrum improved significantly when one hfs constant was fixed at the experimental value of 0.046 mT while the other was allowed to vary. The final value of 0.052 mT for H_c when combined the other fitted and experimentally derived parameters simulate the observed EPR spectrum satisfactorily.[11] The fitted parameters are tabulated in the final column of Table 4.

The ENDOR signals of the two largest hfs constants split into two resonances at low temperatures in either THF or 1,2-dimethoxyethane. This observation prompted us to undertake a temperature dependent study of the proton resonant frequencies and their corresponding line widths. As the temperature was raised from the freezing point, the split signal reduced to one at 210 K, the coalescence temperature. In addition, the line width of an individual ENDOR resonance line of the two largest hfs, generally broadened as the coalescence temperature was approached from either side. These observations are consistent with an intramolecular jump process in which a molecule undergoes dynamic motion, such as chemical exchange or torsion about a bond.[12] In such a case, it is typical to observe at higher temperatures a single, average value of the hfs constant, while at lower temperatures where the rate of exchange is slow, two distinct hfs constants are observed whose average value corresponds to the fast exchange limit. Simplified expressions derived from the modified Bloch equations can be used to determine the chemical rate constant *k* at different temperatures.[12,13] The regions of fast ($k \gg 2\pi\delta\nu_o$) and slow ($k \ll 2\pi\delta\nu_o$) exchange refer to the magnitude of *k* relative to the difference between the two resonance frequencies, $\delta\nu_o = \nu_a - \nu_b$, on one side of the proton Larmor frequency. For a quantitative determination of the rate constants, the unsaturated line width in the absence of exchange must be determined. In addition to a saturation study of the NMR transition with respect to Rf power, it is helpful to use a nearby resonance line that is not affected by the exchange process to estimate the unsaturated line width.[12] The lack of a nearby unaffected resonance line and low signal-to-noise prevents quantitative evaluation of the rate constants in this study. However, assuming that the unsaturated peak-to-peak line width is 150 kHz, a value between the modulation depth (100 kHz) and the narrowest measured line width (206 kHz at 243 K), it is estimated from a plot of ln(*k*) vs $1/T$ that the activation energy E_a for the jump process is approximately 17 kJ/mol.

Discussion

In dilute solution, a radical anion salt can exist as contact ion pairs, solvent separated pairs, and free ions. The extent to which each species forms depends on a number of factors such as the cation, solvent, temperature, concentration, and nature of the electron acceptor. The optical, NMR, and ^{1}H-ENDOR spectra demonstrate that the electron donating ability of the pyrazine and pyridine nitrogen lone pairs of dpq stabilize the contact ion pair in solution throughout the temperature range of this study. Indeed, the crystal structures of both radical anion salts show that K^+ preferentially binds to these nitrogen atoms. In addition, since there are two bidentate sites per dpq molecule,

cation exchange between these two strong binding sites provides a plausible explanation for the splitting of the proton resonances in the ENDOR spectra. Similar examples of intramolecular cation exchange have appeared in the literature.[14] Cation exchange between contact ion pairs is less likely because of the low concentration of the radical anion, <1 mmol, used in the ENDOR experiments. In addition, there was no EPR spectroscopic evidence for the formation of dimers or clusters in frozen solutions based on the absence of resonances ascribable to $\Delta M_s = \pm 1$ or $\Delta M_s = 2$ transitions typical of electronic states in which $S \geqslant 1$. If the same jump process occurs for the parent compound, diphenylquinoxaline, the rate of chemical exchange must be faster than the NMR time scale because only one set of ^{1}H-ENDOR signals was observed at 200 K.[4] Although two nitrogen atoms per binding site affects the affinity for the cation, the electronic structure of the anion is not signifcantly affected when the dpq hfs constants are compared to those of diphenylquinoxaline. In fact, the hfs constants of the quinoxaline protons $H_{5,8}$ and $H_{6,7}$ and pyrazine nitrogens are similar throughout a series of quinoxaline derivatives.[4,9]

The two radical anion salts, K[(dpq)](THF)$_2$ and K[(dpq)]-(MeNH$_2$)$_3$, form linear chains and dimers, respectively. In principle, these structures might facilitate exchange coupling between the unpaired electron spins especially since the spin density is largest at the pyrazine nitrogens. Magnetic susceptibility measurements demonstrate that the coupling is weakly antiferromagnetic in nature for both salts. The Weiss constant measured for K[(dpq)](THF)$_2$, $\theta = -11.8$ K, is an order of magnitude larger than the value obtained for K[(dpq)](MeNH$_2$)$_3$, $\theta = -1.8$ K and may reflect the nearly linear contacts between cations and anions in that crystal. Nevertheless, the overall interaction between spins on adjacent molecules is weak for both materials and probably reflects the large intermolecular distance (>6.0 Å) between radical anions in the crystal and the inability of K^+ to act as an exchange coupling unit.

Experimental Section

General Comments. Solvents were prepared by distillation from the appropriate drying reagent before use. Standard techniques for the low temperature and vacuum line preparation, transfer, storage, and characterization of these reactive materials were employed.[7] dpq was prepared by a modified method of Goodwin and Lions,[15] sublimed at 80 °C onto a water cooled cold finger at 10^{-2} Torr before use, and characterized by ^{1}H NMR spectroscopy, EI-MS, and microanalytical analysis. ^{1}H NMR spectra were recorded on a Varian VXR-300 FT NMR spectrometer.

EPR and ENDOR spectra were recorded on a Bruker ESP300E spectrometer equipped with a DICE ENDOR unit. Typical conditions for EPR were modulation frequency 100 kHz, modulation amplitude 0.1 gauss, power 0.1 mW, and gain 10^5. Typical conditions for ENDOR were modulation frequency 12.5 kHz, microwave power 20−32 mW, radio frequency power 200−300 W, modulation depth 100 kHz, and gain 10^5. Solutions for electrochemical, optical, and EPR measurements were prepared by using a K-cell[7a] fitted with a third chamber that was either an electrochemical or optical cell, or a Suprasil quartz EPR tube as appropriate. Optical spectra were recorded with a Guided Wave Model 260 fiber optic spectrophotometer. Cyclic voltammograms were recorded on a BAS CV-50W voltammetric analyzer with a silver wire as a pseudoreference electrode. A THF solution of the sample (1 mmol) with [(*n*-Bu)$_4$N](PF$_6$) (100 mmol) as supporting electrolyte was used. A sweep rate of 0.1 V/s was used and 100% IR compensation was achieved before each run. The final results were calibrated to ferrocene/ferrocinium. Magnetic susceptibilities of crushed polycrystalline samples were determined with S.H.E. 800 Series and Quantum Design MPMS2 SQUID magnetometers. Corrections for the diamagnetism of K[(dpq)](THF)$_2$ and the sample holder were made by allowing the sample to decompose in the magnetometer and acquiring the background susceptibility. For K[(dpq)]-(MeNH$_2$)$_3$, Pascal's constants were used to estimate the diamagnetic correction of the sample, while the sample holder was run separately. Errors introduced into the susceptibility data by using separate runs for the sample and holder were compensated by a small temperature independent paramagnetic correction that improved the fit of χ_m for K[(dpq)](MeNH$_2$)$_3$.

Preparation of K[(dpq)](THF)$_2$. In a helium-filled glovebox a modified two-chamber K-cell was charged with dpq (284 mg, 1.0 mmol) in one chamber and potassium metal (40 mg, 1.02 mmol) in the sidearm of a second chamber. The cell was then attached to a high vacuum line and a potassium metal mirror was prepared by sublimation (at 10^{-5} Torr) of the metal from the sidearm into the second chamber. The K-cell was immersed in a dry ice/isopropanol bath (−60 °C) and previously dried THF (approximately 15 mL) was transferred to the first chamber by low temperature vacuum distillation. The THF solution of dpq was filtered into the chamber with the metal at which point the solution attained a deep magenta color. After about 1 h, the magenta solution was filtered back into the first chamber, pentane (∼10 mL) was distilled into the chamber, and the K-cell was removed from the vacuum line. Deep purple crystals were grown by cooling the two-solvent system in a programmable temperature bath set to reach −80 °C over a 4 h period.

Preparation of K[(dpq)](MeNH$_2$)$_3$. In an identical procedure, dpq (200 mg, 0.70 mmol) and a potassium mirror (28 mg, 0.72 mmol) in methylamine (approximately 25 mL) were reacted at −60 °C. Deep purple-colored crystals were isolated from the single solvent system by decreasing the temperature of a concentrated solution to −80 °C as in the THF system.

Crystal Handling and Analysis. The procedure used to handle these reactive and air-sensitive crystals was similar to those used with alkalides and electrides.[7] Crystals were stored under vacuum at liquid nitrogen temperature until used. In a nitrogen glovebag, the deep purple crystals were transferred onto a cold copper block (kept at ∼−60 °C) and covered with purified octane. A suitable crystal was picked up with a glass fiber that had vacuum grease on its tip and transferred to the diffractometer under a cold N_2 gas stream (−60 °C). X-ray data were collected with the crystal kept in a cold N_2 gas stream (−90 °C).

Due to the relatively poor quality of the data set obtained with K[(dpq)](THF)$_2$, the reflections were processed using SHELX-93 and only potassium atoms were refined anisotropically. Hydrogen atoms were not refined and were allowed to ride on the appropriate carbon atoms. For K[(dpq)](MeNH$_2$)$_3$ the reflections were processed by the software TEXSAN. All non-hydrogen atoms were refined anisotropically. Hydrogen atoms were allowed to ride on the appropriate carbon and hydrogen atoms. A few atoms of methylamine had higher than usual temperature factors, but no disorder was observed. X-ray diffraction data were collected on a Nicolet P3F diffractometer using a locally modified Nicolet LT-1 low temperature system.

Preparation of Optical and EPR Samples. A K-cell, modified by adding a Suprasil quartz EPR tube or optical cell, was charged with a known quantity of dpq in one chamber and a stochiometric amount of potassium to form the 1:1 adduct in the sidearm of the other chamber. A deep magenta solution in

THF was formed as described above. The solution was diluted further with THF and filtered through a frit into the EPR tube or optical cell. The EPR tube was sealed under vacuum while cooled to liquid N_2 temperature.

Acknowledgment. Support for this research was funded in part by the United States Air Force Grant F4 9620-92-J-0523 DEF, NSF Grant DMR-96-10335, and the Center for Fundamental Materials Research of Michigan State University.

Supporting Information Available: Tables of anisotropic thermal parameters, bond distances, bond angles, torsion angles, and general temperature factor expressions for K[(dpq)](THF)$_2$, and K[(dpq)](NMeH$_2$)$_3$. Also included are ^{1}H NMR spectra of dpq in deutero-acetone with increments of NaI added (18 pages). Ordering information is given on any current masthead page.

References and Notes

(1) Baumgarten, M.; Müllen, K. *Electron Transfer I, Radical Ions: Where Organic Chemistry Meets Materials Sciences*; Mattay, J., Ed.; Topics in Current Chemistry 169; Springer-Verlag: Berlin, 1994; pp 3−103.

(2) Jost, W.; Adam, M.; Müllen, K. *Angew. Chem.* **1992**, *104*, 883.

(3) Echegoyen, L.; DeCian, A.; Fischer, J.; Lehn, J.-M. *Angew. Chem., Int. Ed. Engl.* **1991**, *30*, 838.

(4) Bock, H.; Andreas, J.; Nather, C.; Ruppert, K. *Helv. Chim. Acta* **1994**, *77*, 1939.

(5) Crutchley, R. J. Intervalence Charge Transfer and Electron Exchange Studies of Dinuclear Ruthenium Complexes; Advances in Inorganic Chemistry, 41; Academic Press: Orlando, 1994; pp 273−325.

(6) Barqaw, K. R.; Atfah, M. A. *Electrochim. Acta* **1987**, *32*, 597.

(7) (a) Dye, J. L. *J. Phys. Chem.* **1984**, *88*, 3842. (b) Ward, D. L.; Huang, R. H.; Dye, J. L. *Acta Cryst.* **1988**, *C44*, 1374.

(8) Rasmussen, S. C.; Richter, M. M.; Yi, E.; Place, H.; Brewer, K. J. *Inorg. Chem.* **1990**, *29*, 3926.

(9) (a) Carrington, A.; Santos-Veiga, J. *J. Mol. Phys.* **1962**, *5*, 23. (b) Sevenster, A. J. L.; Tabner, B. *J. Org. Mag. Res.* **1984**, *22*, 521. (c) Russell, G. A.; Konaka, R.; Strom, E. T.; Danen, W. C.; Chang, K.-Y.; Kaupp, G. *J. Am. Chem. Soc.* **1968**, *90*, 4646. (d) Pederson, J. A.; Muus, L. T. *Mol. Phys.* **1969**, *16*, 589. (e) Kaim, W. *J. Chem. Soc., Perkin Trans. II* **1984**, 1767.

(10) Dye, J. L.; Nicely, V. A. *J. Chem. Educ.* **1971**, *48*, 443.

(11) Assignment of the H_c proton is tentative. Density functional calculations at the BLYP/6-31g*//HF/3-21g level are qualitatively accurate in reproducing the experimental hfs constants and indicate that $a_{Hc} > a_{Ha}$.

(12) Kurreck, H.; Kirste, B.; Lubitz, W. *Electron Nuclear Double Resonance Spectroscopy of Radicals in Solution*; VCH Publishers, Inc.: New York, 1988.

(13) Gutowsky, H. S.; Holm, C. H. *J. Chem. Phys.* **1956**, *25*, 1228.

(14) (a) Warhurst, E.; Wilde, A. M. *Trans. Faraday. Soc.* **1970**, *66*, 605. (b) Chippendale, J. C.; Warhurst, E. *Trans. Faraday Soc.* **1968**, *64*, 2332.

(15) Goodwin, H. A.; Lions, F. *J. Am. Chem. Soc.* **1959**, *81*, 6415.